
PERGAMON

Journal of the Mechanics and Physics of Solids
51 (2003) 1701–1721

JOURNAL OF THE
MECHANICS AND
PHYSICS OF SOLIDS

www.elsevier.com/locate/jmps

The indentation modulus of elastically anisotropic materials for indenters of arbitrary shape

J.J. Vlassak[a,*], M. Ciavarella[b], J.R. Barber[c], X. Wang[a]

[a] *Division of Engineering and Applied Sciences, Harvard University, 29 Oxford Street, Cambridge, MA 02138, USA*
[b] *Centre of Excellence in Computational Mechanics, Politecnico di Bari, Bari, Italy*
[c] *Department of Mechanical Engineering, University of Michigan, Ann Arbor, MI 48109, USA*

Received 30 January 2003; received in revised form 2 April 2003; accepted 7 April 2003

Abstract

The contact of an indenter of arbitrary shape on an elastically anisotropic half space is considered. It is demonstrated in a theorem that the solution of the contact problem is the one that maximizes the load on the indenter for a given indentation depth. The theorem can be used to derive the best approximate solution in the Rayleigh–Ritz sense if the contact area is a priori assumed to have a certain shape. This approach is used to analyze the contact of a sphere and an axisymmetric cone on an anisotropic half space. The contact area is assumed to be elliptical, which is exact for the sphere and an approximation for the cone. It is further shown that the contact area is exactly elliptical even for conical indenters when a limited class of Green's functions is considered. If only the first term of the surface Green's function Fourier expansion is retained in the solution of the axisymmetric contact problem, a simpler solution is obtained, referred to as the equivalent isotropic solution. For most anisotropic materials, the contact stiffness determined using this approach is very close to the value obtained for both conical and spherical indenters by means of the theorem. Therefore, it is suggested that the equivalent isotropic solution provides a quick and efficient estimate for quantities such as the elastic compliance or stiffness of the contact. The "equivalent indentation modulus", which depends on material and orientation, is computed for sapphire and diamond single crystals.

Keywords: A: Indentation; B: Anisotropic material; Elastic material

* Corresponding author. Tel.: +1-617-496-0424; fax: +1-617-496-0601.
E-mail address: vlassak@esag.harvard.edu (J.J. Vlassak).

0022-5096/03/$ - see front matter © 2003 Elsevier Ltd. All rights reserved.
doi:10.1016/S0022-5096(03)00066-8

1. Introduction

Indentation measurements are often performed on elastically anisotropic materials in order to determine their elastic properties since indentation experiments are straightforward and are frequently the only way to study the mechanical behavior of a material. Hard ceramic materials are sometimes used in calibration procedures for instrumented indentation, because these materials can be indented entirely in the elastic regime (Swadener and Pharr, 2001). These materials, however, are often highly anisotropic elastically and this needs to be taken into account when analyzing experimental results. In particular, it would be useful to develop a simple algorithm or formula to calculate the contact stiffness from the single-crystal elastic constants.

The anisotropic Hertzian contact problem was solved previously through use of double Fourier transforms (Willis, 1966). Vlassak and Nix (1993) defined the indentation modulus, M, of a general anisotropic material through the following equation:

$$S = \frac{\mathrm{d}F}{\mathrm{d}U} = \frac{2}{\sqrt{\pi}} M \sqrt{A}, \tag{1}$$

where F is the applied load, U the approach of the two bodies, and A the projected contact area. The indentation modulus generally depends on the shape of the indenter, although it is independent of indenter geometry under certain conditions of crystal symmetry (Vlassak, 1994). Taking advantage of a formalism developed by Barnett and Lothe (1975), Vlassak and Nix (1993, 1994) obtained simple expressions for the indentation modulus for a flat punch or when the contact area is known a priori to be circular. Recently, this same approach was extended by Swadener and Pharr (2001) to spherical and conical indenters. For isotropic materials and axisymmetric geometries, M reduces to the plane-strain elastic modulus

$$M = \frac{E}{1 - \nu^2}, \tag{2}$$

independent of indenter shape. For general anisotropic materials, no such straightforward formula is available.

In this paper, we generalize a theorem due to Barber (1974), that provides a method for determining contact area and compliance for isotropic materials (Barber and Billings, 1990). This theorem is shown to apply to a large class of anisotropic materials. The theorem can be used to derive approximate solutions for punches of arbitrary shape. We consider indentation by frictionless conical and spherical (or Hertzian) indenters. Using the theorem, it is shown that the best approximate solution assuming a circular contact area, is a first-order solution that is in essence an equivalent isotropic solution. If the contact area is assumed to be elliptical, the Fourier expansion of the surface Green's function is required, and this expansion is found numerically using a method originally proposed by Barnett and Lothe (1975). Finally, numerical results are presented for the indentation moduli of sapphire and diamond single crystals.

2. The Green's function for an anisotropic half space

A convenient expression for the surface Green's function was derived by Barnett and Lothe (1975) using a technique based on the Stroh formalism for anisotropic materials. Consider a coordinate system $(x_1; x_2; x_3)$. Let $\mathbf{t}$ be an arbitrary unit vector in an infinite anisotropic medium, and let $\mathbf{m}$ and $\mathbf{n}$ be two vectors perpendicular to $\mathbf{t}$, so that $\mathbf{m}; \mathbf{n}; \mathbf{t}$ form a right-hand Cartesian system. We define the matrix $\mathbf{B}(\mathbf{t})$ as

$$B_{js}(\mathbf{t}) = B_{sj}(\mathbf{t}) = \frac{1}{8\pi^2} \int_0^{2\pi} \{(\mathbf{mm})_{js} - (\mathbf{mn})_{jk}(\mathbf{nn})^{-1}_{kr}(\mathbf{nm})_{rs}\} \, \mathrm{d}\varphi, \tag{3}$$

where φ is the angle between $\mathbf{m}$ and some fixed datum in the plane perpendicular to $\mathbf{t}$ (see Fig. 1a). Repeated indices imply a summation over the repeated index from 1 to 3. The matrices $(\mathbf{ab})$ are given by

$$(\mathbf{ab})_{jk} = a_i C_{ijkm} b_m \tag{4}$$

and C_{ijkm} are the elastic stiffness coefficients of the anisotropic material given in the coordinate system $(x_1; x_2; x_3)$. The matrix $\mathbf{B}$ depends only on the elastic constants of the material and the direction $\mathbf{t}$, is symmetric and positive definite.

Now, consider an anisotropic half space with its surface through the origin of the coordinate system (Fig. 1b). The orientation of the boundary of the half space is arbitrary with respect of the coordinate system and is characterized by the direction cosines $(\alpha_1; \alpha_2; \alpha_3)$ of the normal to that boundary. If a concentrated unit load is applied at the origin and perpendicular to the boundary of the half space, the displacement, $w(\mathbf{y})$, in the direction of the load of a point P in the surface of the half space is given by the following Green's function (Vlassak and Nix, 1994):

$$w(\mathbf{y}) = \frac{1}{8\pi^2 |\mathbf{y}|} \left[\alpha_k B^{-1}_{km} \left(\frac{\mathbf{y}}{|\mathbf{y}|} \right) \alpha_m \right] = \frac{h(\theta)}{r}, \tag{5}$$

where $\mathbf{y}$ is the position vector of P. Thus, the displacement of any point in the surface of a half space under the influence of a point load is inversely proportional to the distance, r, to the point load. The angle-dependent part of the surface Green's function, $h(\theta)$ can be readily calculated through numerical integration as indicated by Eq. (3). Since the surface Green's function is periodic in θ, it is often useful to develop $h(\theta)$

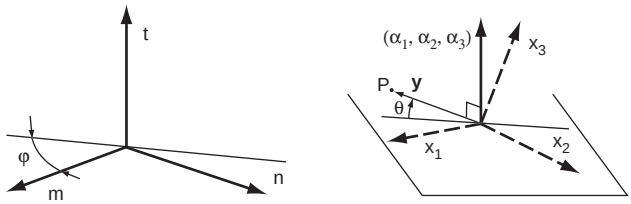

Fig. 1. (a) Schematic representation of the unit vectors used to define the matrix $\mathbf{B}(\mathbf{t})$ for an elastically anisotropic half space. (b) Schematic representation of the vectors involved in the definition of the surface Green's function for an anisotropic half space. The vector $(\alpha_1; \alpha_2; \alpha_3)$ is perpendicular to the surface of the half space, vector $\mathbf{y}$ lies in the surface.

as a Fourier series. In many cases, a few terms in the series are sufficient to obtain adequate accuracy. In the remainder of this paper, $h(\theta)$ is considered a given for a particular material and orientation.

3. A Rayleigh–Ritz approximation

Barber (1974) developed a technique for obtaining a Rayleigh–Ritz approximation to the contact area and the load–indentation relation for the indentation of an isotropic half space by an arbitrary indenter. He first showed that for a given indentation, the exact contact area A_c is that which maximizes the indentation force F—i.e.

$$F(A_c) = \max(F(A)), \tag{6}$$

where A is the set of all possible areas (not necessarily connected) on the surface of the half space. A Rayleigh–Ritz approximation can then be sought in a subset of areas A, notably a set of areas for which $F(A)$ is relatively easy to calculate. In the present instance, an appropriate choice would be the set of all elliptical areas, parametrized by major axis a, minor axis b and orientation φ.

The function $F(A)$ can be written down for any area A for which the solution of the corresponding flat punch problem is known. Suppose the contact pressure distribution $p_1(x, y)$ in area A causes a constant unit displacement $u_1(x, y)$ in A and a different distribution $p(x, y)$ produces $u(x, y)$ also in A. Applying Betti's reciprocal theorem to these two stress states, we obtain

$$\iint_A p_1(x, y)u(x, y)\,\mathrm{d}A = \iint_A p(x, y)u_1(x, y)\,\mathrm{d}A = \iint_A p(x, y)\,\mathrm{d}A = F(A). \tag{7}$$

Thus, the force $F(A)$ can be written down as a convolution of the flat punch pressure distribution $p_1(x, y)$ and the function $u(x, y)$ describing the shape of the indenting punch. The contact pressure distribution for a flat elliptical punch is given by

$$p_1(x, y) = \frac{p_0}{\sqrt{1 - (x^2/a^2) - (y^2/b^2)}} \tag{8}$$

for both isotropic and anisotropic half spaces, where p_0 is a constant. For the isotropic case, unit indentation requires that

$$p_0 = \frac{\mu}{(1 - \nu)bK(e)}, \tag{9}$$

where $K(e)$ is the complete elliptic integral of the first kind and $e = \sqrt{1 - (b^2/a^2)}$ is the eccentricity of the ellipse. For the anisotropic material defined by the Green's function of Eq. (5), one finds

$$p_0 = \frac{1}{\pi b\alpha(e, \varphi)}, \tag{10}$$

where

$$\alpha(e,\varphi)=\int_0^{\pi}\frac{h(\theta+\varphi)}{\sqrt{1-e^2\cos^2\theta}}\,\mathrm{d}\theta \tag{11}$$

and φ is the angle between the major axis of the ellipse and the reference direction for the function h. The result of Eq. (6) was established by Barber (1974) only for the case of isotropic materials, but the argument can be extended to generally anisotropic materials provided they satisfy the condition that the maximum normal indentation at the surface of the half space must occur in a loaded area. At the point of maximum displacement, we must have

$$\nabla^2_{(2)}u\equiv\frac{\partial^2 u}{\partial x^2}+\frac{\partial^2 u}{\partial y^2}<0, \tag{12}$$

where $\nabla^2_{(2)}$ is the two-dimensional Laplacian operator in the surface plane. This quantity is invariant under coordinate transformation in the plane. The Green's function defined in Eq. (5) satisfies this condition at all points other than the origin if

$$\begin{aligned}&\nabla^2_{(2)}\left(\frac{h(\theta)}{r}\right)\\&=\left(\frac{\partial^2}{\partial r^2}+\frac{1}{r}\frac{\partial}{\partial r}+\frac{1}{r^2}\frac{\partial}{\partial\theta^2}\right)\left(\frac{h(\theta)}{r}\right)\\&=2\frac{h(\theta)}{r^3}-\frac{h(\theta)}{r^3}+\frac{h''(\theta)}{r^3}<0\end{aligned} \tag{13}$$

and hence

$$h''(\theta)+h(\theta)<0\quad\text{for all }\theta. \tag{14}$$

If this condition is satisfied, it follows from superposition or convolution that Eq. (12) will be satisfied at all unloaded points for a more general distribution of normal pressure on the half space. Eq. (14) is a necessary condition for the maximum displacement to occur outside of the contact area. Thus,

$$h''(\theta)+h(\theta)\geqslant 0\quad\text{for all }\theta \tag{15}$$

is a sufficient condition for the maximum to occur within the contact area. Many naturally occurring anisotropic materials satisfy Eq. (15) and hence permit Barber's method to be used to determine a Rayleigh–Ritz approximation for the general indentation problem. [1]

[1] This proof can be extended to a larger class of anisotropic materials by defining a general linear coordinate transformation through $X=Ax+By$; $Y=Cx+Dy$. In the new space so defined, it is clear that the inverse dependence of Green's function Eq. (5) on r will be preserved, so that $w=H(\phi)/R$, where $R=\sqrt{X^2+Y^2}$ and ϕ has a one-to-one correspondence with θ. If the transformation constants A;B;C;D can be chosen so as to make the transformed function $H(\phi)$ satisfy Eq. (15), we can conclude that the maximum displacement in the transformed space must occur in a loaded region and hence so must that in the untransformed space.

Assuming Eq. (15) is satisfied for the elastic material, the force $F(A)$ required to establish an elliptical contact area can be written down from Eqs. (7) and (8) as

$$F(A) = \iint_A \frac{p_0 u(x,y)\,\mathrm{d}x\,\mathrm{d}y}{\sqrt{1-(x^2/a^2)-(y^2/b^2)}} \tag{16}$$

where p_0 is given by Eq. (9) for isotropic and Eq. (10) for anisotropic materials. The best elliptical fit to the actual contact area is then obtained by minimizing $F(A)$, by enforcing the conditions

$$\frac{\partial F}{\partial a} = 0; \quad \frac{\partial F}{\partial b} = 0; \quad \frac{\partial F}{\partial \varphi} = 0. \tag{17}$$

4. Solution for conical indenters

If the half space is indented by a circular cone, the displacement imposed by the indenter is given by

$$u(x,y) = U - C\sqrt{x^2+y^2}, \tag{18}$$

where U is a rigid body displacement and C is the cotangent of the cone angle. If the contact area between half space and indenter is assumed to be elliptical, an approximate solution can be derived using Barber's theorem. Substituting $u(x,y)$ into Eq. (16) yields the following expression for the load on the indenter:

$$F(A) = p_0 \iint_A \frac{U - C\sqrt{x^2+y^2}}{\sqrt{1-(x^2/a^2)-(y^2/b^2)}}\,\mathrm{d}x\,\mathrm{d}y. \tag{19}$$

To simplify the integration in Eq. (19), we perform a change of variables

$$\xi = \frac{x}{a}, \quad \eta = \frac{y}{b}, \quad x = a\xi, \quad y = b\eta, \quad \mathrm{d}x = a\,\mathrm{d}\xi, \quad \mathrm{d}y = b\,\mathrm{d}\eta,$$

which converts the domain of integration into the unit circle A_1 and we find

$$F(a,b,\varphi) = p_0 ab \iint_{A_1} \frac{U - C\sqrt{a^2\xi^2 + b^2\eta^2}}{\sqrt{1-\xi^2-\eta^2}}\,\mathrm{d}\xi\,\mathrm{d}\eta. \tag{20}$$

Changing to polar coordinates,

$$\xi = \rho\cos\theta, \quad \eta = \rho\sin\theta, \tag{21}$$

results in

$$F(a,b,\varphi) = p_0 ab \int_0^{2\pi}\int_0^1 \frac{U - C\rho\sqrt{a^2\cos^2\theta + b^2\sin^2\theta}}{\sqrt{1-\rho^2}}\,\rho\,\mathrm{d}\rho\,\mathrm{d}\theta. \tag{22}$$

Evaluation of these integrals is tedious, but routine and finally yields the following result:

$$F(a,b,\varphi) = \pi p_0 ab(2U - CaE(e)) = \frac{2Ua - Ca^2E(e)}{\alpha(e,\varphi)}, \tag{23}$$

where $E(e)$ is the complete elliptic integral of the second kind and where Eq. (10) has been used to eliminate p_0. For the conical indenter, dimensional considerations show that the contact area must retain the same eccentricity and orientation for different values of the rigid-body displacement U and that the characteristic length scale a of the contact area must vary linearly with U. This is readily shown to be the case, if the contact area is characterized by the major axis a and the dimensionless parameters e and φ. Taking into account Eq. (23), the first equation in (17) reduces to

$$U - CaE(e) = 0, \tag{24}$$

confirming that a indeed varies linearly with U. Using Eq. (24) to eliminate a from Eq. (23) finally results in

$$F(e,\varphi) = \frac{U^2}{C\alpha(e,\varphi)E(e)}. \tag{25}$$

Thus, the solution for the conical contact is obtained by choosing the parameters e and φ that minimize the product $\alpha(e,\varphi)E(e)$. The contact stiffness for a cone on a half space is then given by

$$S = \frac{\mathrm{d}F}{\mathrm{d}U} = \frac{2}{\sqrt{\pi}}\sqrt{A}\,\frac{1}{\alpha(e,\varphi)(1-e^2)^{1/4}}, \tag{26}$$

where we have used the definition of e and the expression for the surface area of an ellipse, $A = \pi ab$. Comparing this expression with Eq. (1) shows that the indentation modulus of the half space is given by

$$M_{\mathrm{eqv}} = \frac{1}{\alpha(e,\varphi)(1-e^2)^{1/4}}. \tag{27}$$

It should be noted that the solution obtained by minimization of Eq. (25) is approximate in character because the contact area between indenter and half space is assumed to be elliptical. Swadener and Pharr (2001) recently discussed the problem of axisymmetric conical indenters. They suggested that the contact area is exactly elliptical for a general anisotropic material. It is shown in Appendix 1 that the pressure distribution used by these authors results in an indentation that varies linearly with distance along any straight line radiating from the apex, but that the cross-section of the indentation—i.e., the intersection of the deformed surface with a horizontal plane—is circular only if the anisotropic Green's function of Eq. (5) is of the restricted form $h(\theta) = h_0 + h_{c1}\cos(2\theta) + h_{s1}\sin(2\theta)$, where h_0, h_{c1}, and h_{s1} are constants. The pressure distribution assumed by Swadener and Pharr (2001) does not define the exact solution of the problem for more general anisotropic materials. Hence, the current approach based on Barber's theorem is preferable over the solution presented by Swadener and Pharr, since it provides the best solution in the Rayleigh–Ritz sense.

5. The best circular approximation for a conical indenter

An even simpler approximate solution for conical indenters appropriate for weakly anisotropic materials is obtained if the contact area is restricted to a circular area of

radius a. In this case, the orientation angle φ is arbitrary and the eccentricity vanishes, so that

$$\alpha(0,\varphi) = \int_0^{\pi} h(\theta)\,\mathrm{d}\theta = \pi h_0, \tag{28}$$

where h_0 is the first, θ-independent term in a Fourier series representation of the function $h(\theta)$. Eqs. (25) and (28) then lead to the following simple expression for the force on the indenter:

$$F(a) = \frac{2U^2}{\pi^2 C h_0} = \frac{Ca^2}{2h_0}, \tag{29}$$

since $E(0) = \pi/2$. The indentation modulus of the half space is then given by

$$M_{\mathrm{eqv}} = \frac{1}{\pi h_0}. \tag{30}$$

Thus, if the contact area is assumed to be circular, the indentation modulus depends only on the first-order term of the Fourier series expansion of Green's function. This result can be generalized for indenters of arbitrary shape as discussed in the next section.

6. The equivalent isotropic solution for general indenters

If a circular contact area is assumed, $a = b$, $e = 0$, and Eq. (16) is greatly simplified, not just for conical indenters, but also for indenters described by the general shape function $f(x,y)$:

$$\begin{aligned} F(A) &= \frac{1}{\pi b \alpha(e,\varphi)} \iint_A \frac{u(x,y)\,\mathrm{d}x\,\mathrm{d}y}{\sqrt{1-(x^2/a^2)-(y^2/b^2)}} \\ &= \frac{1}{a\pi^2 h_0} \iint_A \frac{U - f(x,y)\,\mathrm{d}x\,\mathrm{d}y}{\sqrt{1-(r^2/a^2)}}, \end{aligned} \tag{31}$$

where $r = \sqrt{x^2 + y^2}$, and $\alpha(e,\varphi)$ has reduced to πh_0. This equation simply expresses that "the best circular approximate solution in the Rayleigh–Ritz sense corresponds exactly to the solution for an isotropic half space, if $1/\pi h_0$ is taken as the equivalent isotropic indentation modulus, where h_0 is the first term of the Fourier expansion of the surface Green's function $h(\theta)$ of the anisotropic solid". This definition of indentation modulus coincides with that given by Vlassak and Nix (1994) and is in effect that for a flat punch with a circular cross-section. If the geometry of the indenter is axisymmetric, the best circular solution in the Rayleigh–Ritz sense is the exact solution for the corresponding isotropic material.

For the general *non-axisymmetric* contact problem, two types of approximation can be made. First, one can assume that the contact area is circular as discussed in the previous paragraph. In this case, terms of higher order than one in the Fourier expansion of the Green's function do not contribute to the solution. Alternately, one can truncate the Fourier expansion after the constant term, and allow for elliptical contact areas

(an alternative, non-elliptical solution is also possible using the Fabrikant method as exposed in Barber and Billings, 1990). This solution is referred to as the equivalent isotropic solution. Since the equivalent isotropic solution is more general than the solution assuming a circular contact area, it is also more accurate, especially for indenters with an elongated geometry. It degenerates to the solution with the circular contact area if the indenter geometry is axisymmetric. The equivalent isotropic solution for axisymmetric indenters is completely determined by the indentation modulus defined in Eq. (30). Using the equivalent isotropic approximation, the Barber and Billings (1990) procedure can be applied to any indenter geometry of interest.

In the general anisotropic solution with an elliptical contact area, all terms of the Fourier expansion for $h(\theta)$ are required in order to maximize $F(A)$. In the next section, two specific examples are discussed, i.e., indentation of sapphire and diamond by an axisymmetric cone and by a spherical indenter, and the results are compared to the equivalent isotropic solution. A more detailed analysis of the spherical contact problem is presented in Appendix 2.

7. Application

The theorem discussed in the first part of this paper will now be applied to the indentation of single-crystalline sapphire and diamond. Sapphire is commonly used in instrumented indentation experiments for calibration of the indenter tip shape (Oliver and Pharr, 1992). Since sapphire is anisotropic, it is essential to use the correct indentation modulus to obtain an accurate calibration of the indenter shape. The point group of sapphire is $\bar{3}m$ and single-crystalline sapphire has six independent elastic constants. The adiabatic elastic constants were measured by Wachtman et al. (1960) and are as follows: $(C_{11}, C_{33}, C_{44}, C_{12}, C_{13}, C_{14}) = (496.8, 498.1, 147.4, 163.6, 110.9, -23.5)$ GPa, where the x_1 and x_3 axes are aligned with the a- and c-axis of the crystal, respectively. The elastic constants under isothermal conditions, which are more relevant to most indentation experiments, differ from the adiabatic values by less than 1%.

Fig. 2 shows the indentation modulus of single-crystalline sapphire calculated from the equivalent isotropic solution using Eq. (30). Since the indenter is assumed to be axisymmetric, the shape of the contact area is circular. At this level of approximation, the indentation modulus coincides exactly with that for a flat circular punch. The indentation modulus is plotted as a function of the angle between the surface normal and the sapphire basal plane. Three cases are considered: the surface normal lies in the a–c crystal plane ($\alpha = 0$), the surface normal lies in the plane through the c-axis making an angle of -30° with the a–c plane ($\alpha = -30^\circ$), and the surface normal lies in the plane through the c-axis at an angle of $+30^\circ$ with the a–c plane ($\alpha = +30^\circ$). According to Wachtman et al. (1960), directions in the latter two planes show extreme values of Young's modulus and one can reasonably expect extreme values for the indentation modulus as well. This is indeed borne out in Fig. 2 where the indentation modulus takes on extreme values for directions with $\alpha = -30^\circ$ and $+30^\circ$. It should be noted, however, that the orientations of the extremes do not coincide exactly with those for Young's modulus. The maximum variation of the indentation modulus with orientation

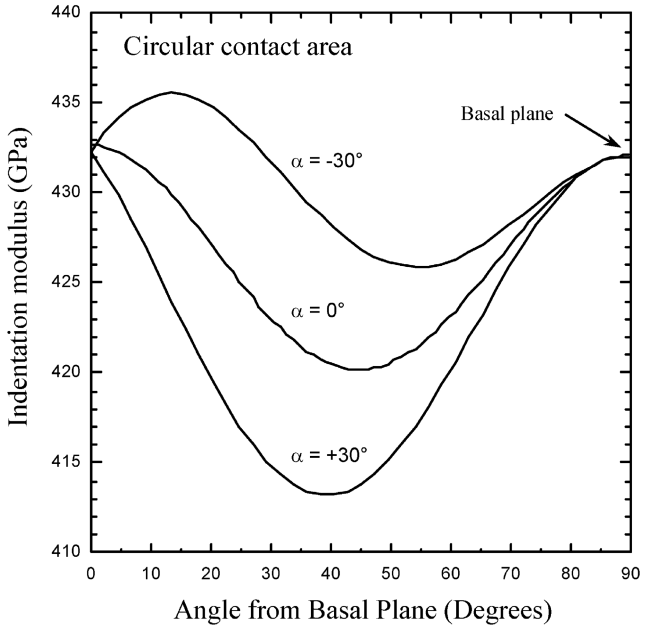

Fig. 2. Indentation modulus of single-crystalline sapphire for a circular contact area.

is approximately 5% and the indentation modulus for the basal plane, which is most commonly used for indentation calibration purposes, is 432 GPa.

Fig. 3 depicts the indentation moduli of sapphire for conical and spherical indenters calculated from the general anisotropic solution assuming the contact area is elliptical. These are exact results for both spherical and conical indenters. The difference between the indentation modulus for conical and spherical indenters is less than 0.03% and it is nearly impossible to distinguish both curves in Fig. 3. The results are in very good agreement with data presented by Swadener and Pharr (2001). A comparison of the results in Figs. 2 and 3 shows that the difference between the indentation modulus for a conical or a spherical indenter and that for a flat punch with a circular cross-section is extremely small. The error involved in using the flat punch solution is at most 0.1%, which is in general significantly smaller than the uncertainty in the elastic constants.

Figs. 4a and b show the ratio a/b for indentation with a conical and a spherical indenter, respectively. The degree of eccentricity of the contact areas is small for all orientations, and somewhat larger for cones than for spheres in agreement with an observation made by Swadener and Pharr (2001). The results for $\alpha = -30^\circ$ and $+30^\circ$ agree very well with the results presented by these authors, but there is a rather large discrepancy for $\alpha = 0$. The results for $\alpha = 0$ plotted in Figs. 4a and b are in line with the symmetry properties of the Green's functions for these orientations. The contact area for indentation in the basal plane is circular and the indentation modulus is independent

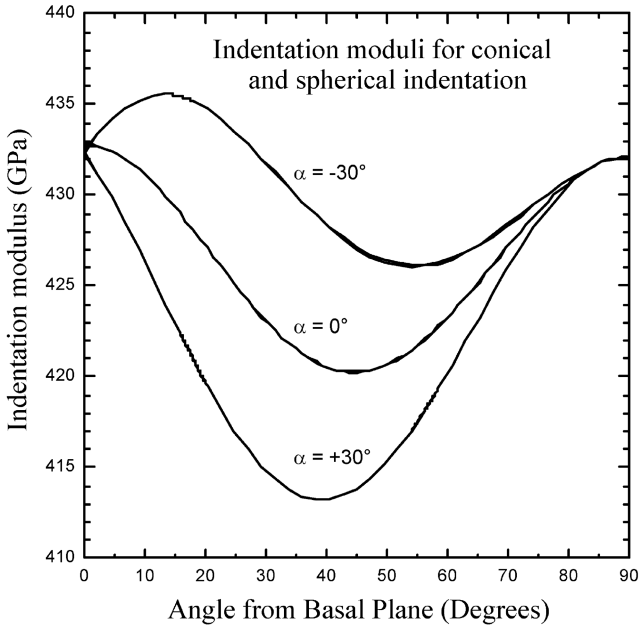

Fig. 3. Indentation modulus of single-crystalline sapphire for conical or spherical indentation. The difference between the moduli for the two types of indenter is too small to be distinguished on the graph.

of α The ratio a/b presented in Fig. 4a also agrees very well with Eq. (A.19), which gives the aspect ratio if the Green's function is truncated after the first-order terms.

Fig. 5 depicts the orientation of the contact ellipses for conical and spherical indenters, respectively. Note that the orientation of the contact ellipse is exactly the same for both conical and spherical indenters as pointed out by Swadener and Pharr (2001). Since the planes at $\alpha = -30°$ and $+30°$ are mirror planes in sapphire, symmetry requires that one of the main axes of the contact ellipse lie in the mirror plane, i.e., $\varphi = 0°$ or 90°. The plane at $\alpha = 0$, on the other hand, has no particular symmetry properties other than a twofold axis perpendicular to the c-axis, and the inclination of the contact ellipse can accordingly take on any value between 0° and 180°. Note that the contact ellipse for a surface perpendicular to the a-axis is not aligned with the c-axis. Since sapphire has a center of symmetry, the orientation of the contact ellipse for a surface perpendicular to the a-axis is reversed.

Indenter tips used in depth-sensitive indentation experiments are usually fabricated from diamond single crystals because of their large stiffness. When analyzing experimental results obtained with these indenters, a correction is made to the measurements in order to account for the finite stiffness of the diamond tip. This correction is small for compliant materials, but can be quite significant when testing stiff materials. Since diamond is anisotropic, it is important to take into account the orientation of the diamond tip when making this correction. Fig. 6 shows the indentation modulus for single-crystal diamond as a function of orientation. The elastic constants used in the

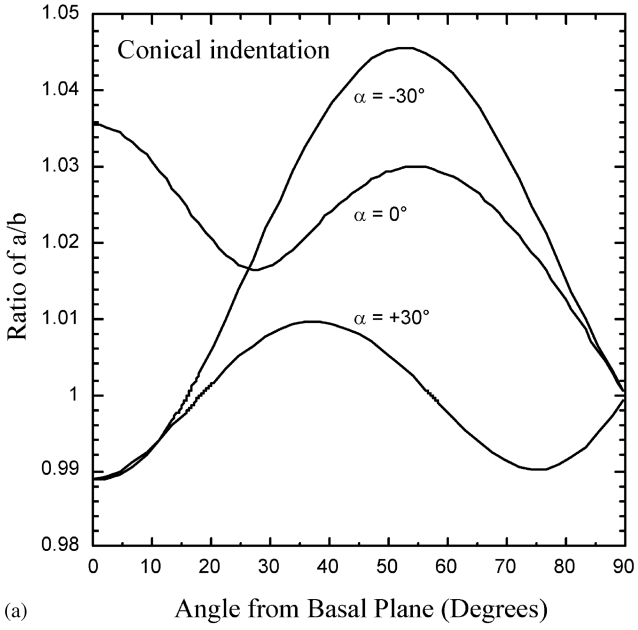

(a)

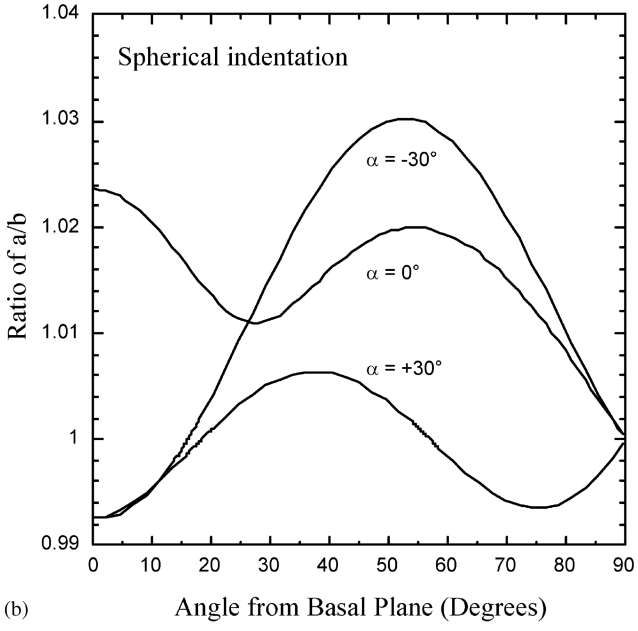

(b)

Fig. 4. (a) Variation of the ratio of the major axes of the contact ellipse with surface orientation for conical indentation of a sapphire single crystal. (b) Variation of the ratio of the major axes of the contact ellipse with surface orientation for spherical indentation of a sapphire single crystal.

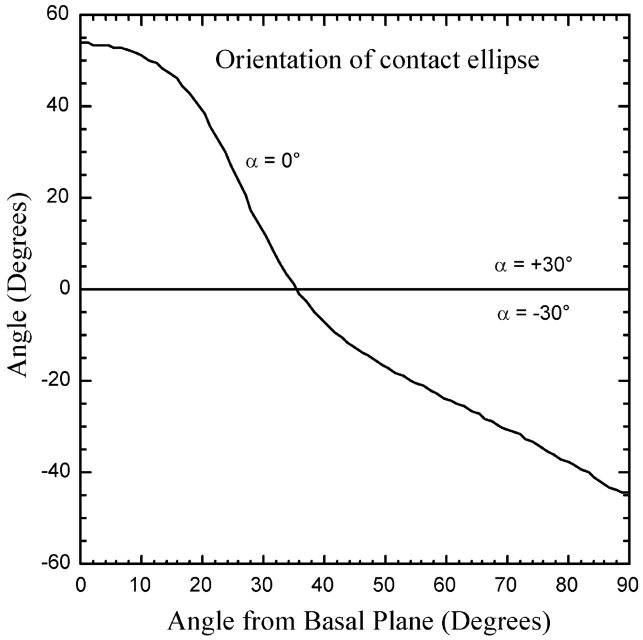

Fig. 5. Variation of the inclination of the contact ellipse with surface orientation for conical and spherical indentation of a sapphire single crystal. The inclination is defined as the angle between the *a*-axis of the ellipse and the intersection of the surface of the half space with the basal plane. The difference between the two types of indenter is too small to be distinguished on the graph.

calculation are the adiabatic constants reported by McSkimin and Bond (1972) and are given by $(C_{11}, C_{12}, C_{44}) = (1079, 124, 578)$ GPa, where the coordinate axes are aligned with the cube axes of the crystal. The calculations are depicted for a conical contact, but the results are indistinguishable from those for spherical indenters. The indentation modulus takes on its maximum value (1165 GPa) when the surface of the half space is an octahedral plane, and its minimum value (1126 GPa) when the surface is a cube plane.

8. Conclusions

We have extended a theorem on the indentation of isotropic materials originally due to Barber (1974) to elastically anisotropic materials. According to this theorem, the exact contact area between an indenter of arbitrary shape and a half space is that which maximizes the indentation force for a given indentation depth. The theorem is used to derive an approximate solution for the indentation of an elastically anisotropic half space by a cone, and a simple method is proposed to determine the orientation and the eccentricity of the contact area between indenter and half space.

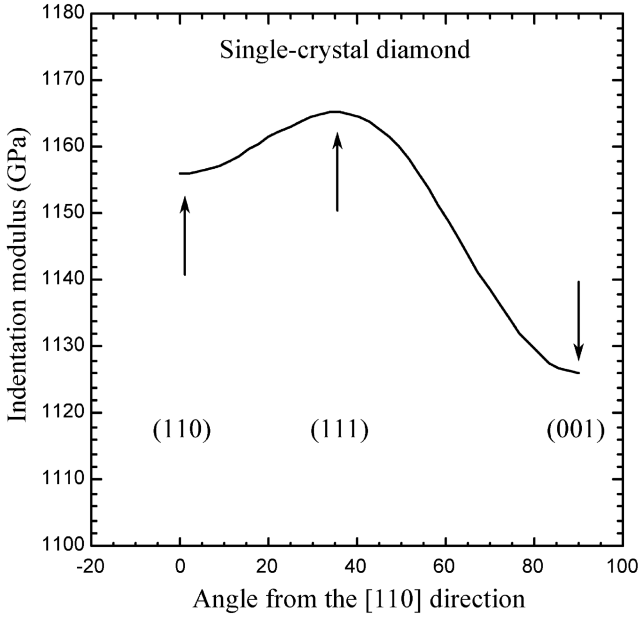

Fig. 6. Variation of the indentation modulus of single crystal diamond with orientation for surfaces belonging to the $[1\,\bar{1}\,0]$ zone. The angle is measured between the surface normal and the [1 1 0] direction. The calculations were performed for conical indentation.

The problem is further simplified through definition of the equivalent isotropic solution where the surface Green's function of the solid is replaced by the first term of its Fourier expansion. The indentation modulus for axisymmetric indenters is then given by $1/\pi h_0$, independent of the actual shape of the indenter. Numerical results show that for a large class of anisotropic materials use of the indentation modulus so defined is indeed justified as long as the indenter is axisymmetric. This definition coincides with the indentation modulus defined earlier by Vlassak and Nix (1994) for flat punches and greatly simplifies the calculation of the contact stiffness of an indenter on an anisotropic half space.

The indentation moduli of single-crystalline sapphire and diamond were calculated for a number of surface orientations using the new approach. Results are in good agreement with previously published data and with the *exact* solution obtained for a conical contact if the Green's function is truncated after the first-order terms.

Acknowledgements

The authors would like to acknowledge funding from the National Science Foundation, CAREER Award DMR-0133559 (JJV), as well as support from the Ministry of Italian Research for the Centre of Excellence in Computational Mechanics (MC).

Appendix A. Indentation of an anisotropic half space by a rigid cone

The normal surface displacement u_z at the point $Q(x, y)$ inside the contact area due to a pressure distribution $p(x', y')$ is

$$u_z = \int_0^{\pi} \int_A^B p(x', y') h(\theta + \varphi)\, \mathrm{d}r\, \mathrm{d}\theta, \tag{A.1}$$

where φ is the angle between the x-axis and the reference direction for the Green's function $h(\theta)$, A, B are the points where a line through Q inclined at angle θ intersects the edge of the contact area, and r is the distance between the points $Q(x, y)$ and $P(x', y')$.

Following Swadener and Pharr (2001), we consider the case where $p(x', y')$ is of the form

$$p(x', y') = p_0 \cosh^{-1}\left(\frac{x'^2}{a^2} + \frac{y'^2}{b^2}\right)^{-1/2}, \tag{A.2}$$

acting over the ellipse $(x'^2/a^2) + (y'^2/b^2) < 1$. From geometrical considerations, we have

$$x' = x - r\cos\theta, \quad y' = y - r\sin\theta. \tag{A.3}$$

Substituting Eqs. (A.2) and (A.3) into Eq. (A.1) and performing the inner integration, we obtain

$$u_z(x, y) = \pi ab\, p_0 \left(\int_0^{\pi} \frac{h(\theta + \varphi)\, \mathrm{d}\theta}{\sqrt{b^2 \cos^2\theta + a^2 \sin^2\theta}} - \rho \int_0^{\pi} \frac{|\sin(\theta - \phi)| h(\theta + \varphi)\, \mathrm{d}\theta}{b^2 \cos^2\theta + a^2 \sin^2\theta} \right), \tag{A.4}$$

where ρ, ϕ are the polar coordinates of Q—i.e.,

$$x = \rho\cos\phi, \quad y = \rho\sin\phi. \tag{A.5}$$

The first term in Eq. (A.4) represents a rigid body displacement and the second is a linear function of ρ, the multiplier of which is a function of ϕ. This will represent the indentation due to an axisymmetric cone if and only if the integral

$$I(\phi) \equiv \int_0^{\pi} \frac{|\sin(\theta - \phi)| h(\theta + \varphi)\, \mathrm{d}\theta}{b^2 \cos^2\theta + a^2 \sin^2\theta}, \tag{A.6}$$

is independent of ϕ for all ϕ. This integral can be evaluated by expanding the functions $|\sin(\theta - \phi)|$ and $h(\theta + \varphi)$ as Fourier series. Maxwell's reciprocal theorem requires that the Green's function must satisfy the condition $h(\theta + \pi) = h(\theta)$ and hence the Green's function can be expanded as a Fourier series in terms of the angle (2θ) as

$$h(\theta) = h_0 + \sum_{n=1}^{\infty} h_{cn} \cos(2n\theta) + \sum_{n=1}^{\infty} h_{sn} \sin(2n\theta). \tag{A.7}$$

It follows directly that

$$h(\theta+\varphi)=h_0+\sum_{n=1}^{\infty}[h_{cn}\cos(2n\varphi)+h_{sn}\sin(2n\varphi)]\cos(2n\theta)$$
$$+\sum_{n=1}^{\infty}[h_{sn}\cos(2n\varphi)-h_{cn}\sin(2n\varphi)]\sin(2n\theta). \tag{A.8}$$

We also obtain

$$|\sin(\theta-\phi)|=\frac{2}{\pi}-\frac{4}{\pi}\sum_{m=1}^{\infty}\frac{[\cos(2m\theta)\cos(2m\phi)+\sin(2m\theta)\sin(2m\phi)]}{4m^2-1}. \tag{A.9}$$

Using Gradshteyn and Ryzhik 3.613, we can show that

$$\int_0^{\pi}\frac{\cos(2j\theta)\,\mathrm{d}\theta}{b^2\cos^2\theta+a^2\sin^2\theta}=\frac{\pi}{ab}\left(\frac{a-b}{a+b}\right)^j,$$
$$\int_0^{\pi}\frac{\sin(2j\theta)\,\mathrm{d}\theta}{b^2\cos^2\theta+a^2\sin^2\theta}=0,\quad j\geqslant 0 \tag{A.10}$$

and hence

$$\int_0^{\pi}\frac{\cos(2n\theta)\cos(2m\theta)\,\mathrm{d}\theta}{b^2\cos^2\theta+a^2\sin^2\theta}=\frac{\pi}{2ab}\left[\left(\frac{a-b}{a+b}\right)^{|m-n|}+\left(\frac{a-b}{a+b}\right)^{m+n}\right],$$
$$\int_0^{\pi}\frac{\sin(2n\theta)\sin(2m\theta)\,\mathrm{d}\theta}{b^2\cos^2\theta+a^2\sin^2\theta}=\frac{\pi}{2ab}\left[\left(\frac{a-b}{a+b}\right)^{|m-n|}-\left(\frac{a-b}{a+b}\right)^{m+n}\right],$$
$$\int_0^{\pi}\frac{\sin(2n\theta)\cos(2m\theta)\,\mathrm{d}\theta}{b^2\cos^2\theta+a^2\sin^2\theta}=\int_0^{\pi}\frac{\cos(2n\theta)\sin(2m\theta)\,\mathrm{d}\theta}{b^2\cos^2\theta+a^2\sin^2\theta}=0. \tag{A.11}$$

Substituting Eqs. (A.8) and (A.9) into Eq. (A.6) and using Eqs. (A.11), we can evaluate the function $I(\phi)$ as

$$I(\phi)=\frac{2h_0}{ab}-\frac{4h_0}{ab}\sum_{m=1}^{\infty}\left(\frac{a-b}{a+b}\right)^m\frac{\cos(2m\phi)}{4m^2-1}$$
$$+\frac{2}{ab}\sum_{n=1}^{\infty}[h_{cn}\cos(2n\varphi)+h_{sn}\sin(2n\varphi)]\left(\frac{a-b}{a+b}\right)^n$$
$$-\frac{2}{ab}\sum_{m=1}^{\infty}\sum_{n=1}^{\infty}\frac{[h_{cn}\cos(2n\varphi)+h_{sn}\sin(2n\varphi)]\cos(2m\phi)}{4m^2-1}$$

$$\times\left[\left(\frac{a-b}{a+b}\right)^{|m-n|}+\left(\frac{a-b}{a+b}\right)^{m+n}\right]$$

$$-\frac{2}{ab}\sum_{m=1}^{\infty}\sum_{n=1}^{\infty}\frac{[h_{sn}\cos(2n\varphi)-h_{cn}\sin(2n\varphi)]\sin(2m\phi)}{4m^2-1}$$

$$\times\left[\left(\frac{a-b}{a+b}\right)^{|m-n|}-\left(\frac{a-b}{a+b}\right)^{m+n}\right].$$

It is not generally possible to choose b/a and φ to make $I(\phi)$ independent of ϕ. For example, in the simple case

$$h(\theta)=h_0+h_{c2}\cos(4\theta), \tag{A.12}$$

we obtain $\varphi=0$ by symmetry, and

$$I(\phi)=\frac{2h_0}{ab}+\frac{2h_{c2}}{ab}\left(\frac{a-b}{a+b}\right)^2-\frac{4h_0}{ab}\left(\frac{a-b}{a+b}\right)\frac{\cos(2\phi)}{3}-\frac{2h_{c2}}{ab}\frac{\cos(2\phi)}{3}$$

$$\times\left[\left(\frac{a-b}{a+b}\right)+\left(\frac{a-b}{a+b}\right)^3\right]-\frac{4h_0}{ab}\sum_{m=2}^{\infty}\left(\frac{a-b}{a+b}\right)^m\frac{\cos(2m\phi)}{4m^2-1}$$

$$-\frac{2h_{c2}}{ab}\sum_{m=2}^{\infty}\frac{\cos(2m\phi)}{4m^2-1}\left[\left(\frac{a-b}{a+b}\right)^{m-2}+\left(\frac{a-b}{a+b}\right)^{m+2}\right].$$

The terms for $m\geqslant 2$ will be zero if and only if

$$\left(\frac{a-b}{a+b}\right)^{-2}+\left(\frac{a-b}{a+b}\right)^2=-\frac{2h_0}{h_{c2}}, \tag{A.13}$$

whilst the $\cos(2\phi)$ term will be zero only if

$$1+\left(\frac{a-b}{a+b}\right)^2=-\frac{2h_0}{h_{c2}}. \tag{A.14}$$

These two equations cannot be satisfied simultaneously by any choice of b/a. There is an exact solution, however, if $h(\theta)$ is given by

$$h(\theta)=h_0+h_{c1}\cos(2\theta)+h_{s1}\sin(2\theta), \tag{A.15}$$

since in that case $m\geqslant n$ for all the non-zero terms and

$$I(\phi)=\frac{2h_0}{ab}+\frac{2}{ab}[h_{c1}\cos(2\varphi)+h_{s1}\sin(2\varphi)]\left(\frac{a-b}{a+b}\right)$$

$$-\frac{2A}{ab}\sum_{m=1}^{\infty}\left(\frac{a-b}{a+b}\right)^m\frac{\cos(2m\phi)}{4m^2-1}-\frac{2B}{ab}\sum_{m=1}^{\infty}\left(\frac{a-b}{a+b}\right)^m\frac{\sin(2m\phi)}{4m^2-1}, \tag{A.16}$$

where

$$A = 2h_0 + [h_{c1}\cos(2\varphi) + h_{s1}\sin(2\varphi)]\left[\left(\frac{a-b}{a+b}\right)^{-1} + \left(\frac{a-b}{a+b}\right)\right],$$

$$B = [h_{s1}\cos(2\varphi) - h_{c1}\sin(2\varphi)]\left[\left(\frac{a-b}{a+b}\right)^{-1} - \left(\frac{a-b}{a+b}\right)\right]. \tag{A.17}$$

The function $I(\phi)$ will be independent of ϕ, if the aspect ratio b/a and the orientation φ are chosen such that $A = B = 0$. It is always possible to choose the reference axis for $h(\theta)$ such that $h_{s1} = 0$, in which case $B = 0$ is satisfied by the choice of $\varphi = 0$. The remaining condition $A = 0$ then gives

$$2h_0 + h_{c1}\left[\left(\frac{a-b}{a+b}\right)^{-1} + \left(\frac{a-b}{a+b}\right)\right] = 0 \tag{A.18}$$

with solution

$$\frac{b}{a} = \sqrt{\frac{h_0 + h_{c1}}{h_0 - h_{c1}}}. \tag{A.19}$$

For many materials the higher-order Fourier terms are small and this expression is a useful approximation to the eccentricity. In principle, the solution obtained by the Rayleigh–Ritz argument is preferable as an approximation, since it takes into account the full function $h(\theta)$. For the materials discussed in Section 7, however, the difference in b/a calculated using the two approaches is on the order of 0.03% or less.

Appendix B. Indentation of an anisotropic half space by a rigid sphere

The Rayleigh–Ritz analysis for a spherical indenter proceeds exactly as in the conical case, except that the function $u(x, y)$ of Eq. (18) is replaced by

$$u(x, y) = U - C(x^2 + y^2). \tag{B.1}$$

Following the same steps as before, the equivalent of Eq. (22) becomes

$$F(a, b, \varphi) = p_0 ab \int_0^{2\pi}\int_0^1 \frac{(U - C\rho^2(a^2\cos^2\theta + b^2\sin^2\theta))\rho}{\sqrt{1-\rho^2}}\,\mathrm{d}\rho\,\mathrm{d}\theta \tag{B.2}$$

and this is easily evaluated as

$$F(a, b, \varphi) = 2\pi p_0 ab(U - C(a^2 + b^2)/3) = \frac{2a(U - C(a^2 + b^2)/3)}{\alpha(e, \varphi)}. \tag{B.3}$$

We now change variables to a, e, and φ using $b^2 = a^2(1 - e^2)$ and hence

$$F(a, e, \varphi) = \frac{2a(U - Ca^2(2 - e^2)/3)}{\alpha(e, \varphi)}. \tag{B.4}$$

The condition $\partial F/\partial a = 0$ then results in

$$U - Ca^2(2 - e^2) = 0. \tag{B.5}$$

Using this condition to eliminate a yields

$$F(a, e, \varphi) = \frac{4U^{3/2}}{3\alpha(e, \varphi)\sqrt{C(2 - e^2)}}. \tag{B.6}$$

Since it was shown by Willis (1966) that the contact area for a spherical indenter is elliptical, Eq. (B.6) is an exact result. The eccentricity and orientation of the contact area is determined by minimizing the function

$$\alpha(e, \varphi)\sqrt{(2 - e^2)}. \tag{B.7}$$

The indentation modulus for a spherical indenter can be found from Eqs. (B.6), (B.5) and (1) and is given by

$$M = \frac{1}{\alpha(e, \varphi)(1 - e^2)^{1/4}}. \tag{B.8}$$

Note that this is the same expression as for the conical indenter. The exact numerical values of the indentation moduli are slightly different, however, since the eccentricity and orientation for a conical contact is found by minimizing $\alpha(e, \varphi)E(e)$ instead of Eq. (B.7).

It is instructive to consider the simple case where the Green's function $h(\theta)$ contains only two terms:

$$h(\theta) = h_0 - h_{c1}\cos(2\theta). \tag{B.9}$$

Symmetry demands that the contact area be aligned with the axes $\theta = 0,\ \pi/2$. As a result, we can set $\varphi = 0$ and evaluate

$$\alpha(e) = \int_0^{\pi} \frac{h_0 - h_{c1}\cos(2\theta)}{\sqrt{1 - e^2\cos^2\theta}}\,\mathrm{d}\theta = h_0\alpha_0(e) - h_{c1}\alpha_2(e), \tag{B.10}$$

where

$$\alpha_0 = \int_0^{\pi} \frac{\mathrm{d}\theta}{\sqrt{1 - e^2\cos^2\theta}}, \quad \alpha_2 = \int_0^{\pi} \frac{\cos(2\theta)\,\mathrm{d}\theta}{\sqrt{1 - e^2\cos^2\theta}}. \tag{B.11}$$

It then follows that the eccentricity in the Hertzian case is determined by the equation

$$h_0\frac{\partial}{\partial e}(\alpha_0(e)\sqrt{2 - e^2}) - h_{c1}\frac{\partial}{\partial e}(\alpha_2(e)\sqrt{2 - e^2}) = 0 \tag{B.12}$$

and we can solve this equation inversely by writing

$$\frac{h_{c1}}{h_0} = \frac{(\partial/\partial e)(\alpha_0(e)\sqrt{2 - e^2})}{(\partial/\partial e)(\alpha_2(e)\sqrt{2 - e^2})}. \tag{B.13}$$

In effect, this equation defines the ratio of the 'anisotropic' term h_{c1} to the isotropic term h_0 required to generate a contact area of prescribed eccentricity e.

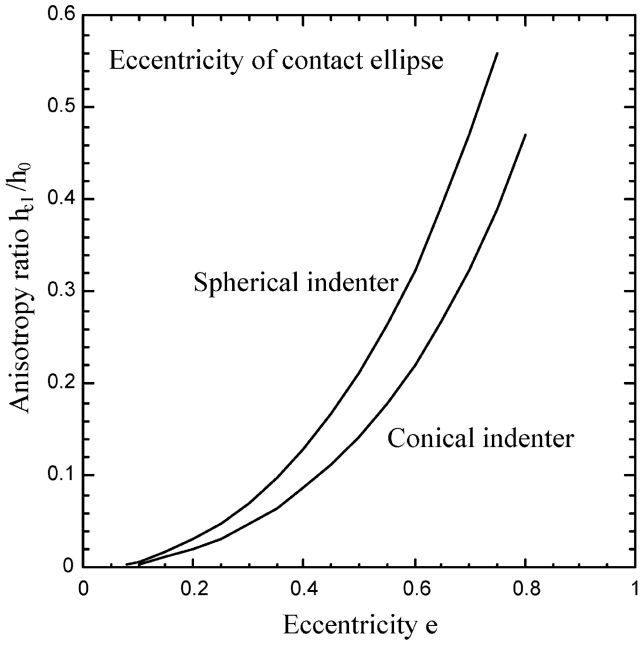

Fig. 7. The ratio h_{c1}/h_0 as a function of the eccentricity of the contact area e.

A similar argument for the conical indenter leads to the condition

$$\frac{h_{c1}}{h_0} = \frac{(\partial/\partial e)(\alpha_0(e)E(e))}{(\partial/\partial e)(\alpha_2(e)E(e))}. \tag{B.14}$$

These two expressions are plotted in Fig. 7 as a function of e. Two features of this figure are significant: A fairly small degree of anisotropy (h_{c1}/h_0) causes significant eccentricity of the contact area and the eccentricity is significantly larger for conical indentation than for indentation by a sphere.

References

Barber, J.R., 1974. Determining the contact area in elastic-indentation problems. J. Strain Anal. 9, 230–232.

Barber, J.R., Billings, D.A., 1990. An approximate solution for the contact area and elastic compliance of a smooth punch of arbitrary shape. Int. J. Mech. Sci. 32, 991–997.

Barnett, D.M., Lothe, J., 1975. Line force loadings on anisotropic half-spaces and wedges. Phys. Norv. 8, 13–22.

McSkimin, H.J., Bond, W.L., 1972. Elastic moduli of diamond as a function of pressure and temperature. J. Appl. Phys. 43, 2944–2948.

Oliver, W.C., Pharr, G.M., 1992. An improved technique for determining hardness and elastic modulus using load and displacement sensing indentation experiments. J. Mater. Res. 7, 1564–1583.

Swadener, J.G., Pharr, G.M., 2001. Indentation modulus of elastically anistropic half-spaces by cones and parabolae of revolution. Philos. Mag. A 81, 447–466.

Vlassak, J.J., 1994. New experimental techniques and analysis methods for the study of the mechanical properties of materials in small volumes, Ph.D. Dissertation, Department of Materials Science, Stanford University.

Vlassak, J.J., Nix, W.D., 1993. Indentation modulus of elastically anisotropic half spaces. Philos. Mag. A 67, 1045–1056.

Vlassak, J.J., Nix, W.D., 1994. Measuring the elastic properties of anisotropic materials by means of indentation experiments. J. Mech. Phys. Solids 42 (8), 1223–1245.

Wachtman Jr., J.B., Tefft, W.E., Lam Jr., D.G., Stinchfield, R.P., 1960. Elastic constants of synthetic single crystal corundum at room temperature. J. Res. Nat. Bur. Stand.—A. Physics and Chemistry 64A, 213–228.

Willis, J.R., 1966. Hertzian contact of anisotropic bodies. J. Mech. Phys. Solids 14, 163–176.